Article

Spring Phenological Responses of Diverse Vegetation Types to Extreme Climatic Events in Mongolia

Qier Mu [1,2], Sainbuyan Bayarsaikhan [1,2,*], Gang Bao [3,4], Battsengel Vandansambuu [1,2], Siqin Tong [3,4], Byambakhuu Gantumur [1,2], Byambabayar Ganbold [1,2] and Yuhai Bao [3,4]

1 Department of Geography, School of Art and Sciences, National University of Mongolia, Ulaanbaatar 14200, Mongolia; 20d1num0113@stud.num.edu.mn (Q.M.); battsengel@num.edu.mn (B.V.); byambakhuu@num.edu.mn (B.G.); byambabayar@num.edu.mn (B.G.)

2 Research Laboratory of Geo-Informatics (GEO-iLAB), Graduate School, National University of Mongolia, Ulaanbaatar 14200, Mongolia

3 Inner Mongolia Key Laboratory of Remote Sensing and Geography Information System, Hohhot 010022, China; baogang@imnu.edu.cn (G.B.); tongsq223@imnu.edu.cn (S.T.); baoyuhai@imnu.edu.cn (Y.B.)

4 College of Geographical Science, Inner Mongolia Normal University, Hohhot 010022, China

* Correspondence: sainbuyan.b@num.edu.mn

Abstract: The increasing frequency of extreme climate events may significantly alter the species composition, structure, and functionality of ecosystems, thereby diminishing their stability and resilience. This study draws on temperature and precipitation data from 53 meteorological stations across Mongolia, covering the period from 1983 to 2016, along with MODIS normalized difference vegetation index (NDVI) data from 2001 to 2016. The climate anomaly method and the curvature method of cumulative NDVI logistic curves were employed to identify years of extreme climate events and to extract the start of the growing season (SOS) in Mongolia. Furthermore, the study assessed the impact of extreme climate events on the SOS across different vegetation types and evaluated the sensitivity of the SOS to extreme climate indices. The study results show that, compared to the multi-year average green-up period from 2001 to 2016, extreme climate events significantly impact the SOS. Extreme dryness advanced the SOS by 6.9 days, extreme wetness by 2.5 days, and extreme warmth by 13.2 days, while extreme cold delayed the SOS by 1.2 days. During extreme drought events, the sensitivity of SOS to TN90p (warm nights) was the highest; in extremely wet years, the sensitivity of SOS to TX10p (cool days) was the strongest; in extreme warm events, SOS was most sensitive to TX90p (warm days); and during extreme cold events, SOS was most sensitive to TNx (maximum night temperature). Overall, the SOS was most sensitive to extreme temperature indices during extreme climate events, with a predominantly negative sensitivity. The response and sensitivity of SOS to extreme climate events varied across different vegetation types. This is crucial for understanding the dynamic changes of ecosystems and assessing potential ecological risks.

Keywords: spring phenology; climate anomaly; extreme climate events; extreme climate indices; diverse vegetation types; sensitivity

1. Introduction

Under the backdrop of global warming, the likelihood of climate anomalies and extreme climate events is increasing [1]. Extreme climate events and trends have received more attention due to their greater sensitivity to climate change compared to average climate changes [2–5]. Climate anomalies refer to significant deviations from the average climate value for a specific period, and extreme climate events are defined as instances where climate variables exceed (or fall below) certain thresholds, approaching the upper (or lower) limits of the observed range for that variable [6].Although they are low-probability

events, extreme climate changes have a greater impact on ecosystem functions and productivity than average climate changes [3,7,8]. The 27 extreme climate indicators that have been recommended by the Expert Team on Climate Change Detection and Indices are frequently utilized in studies related to extreme climate change [9,10]. Many scholars have conducted extensive research on extreme climate changes [11–15]. Liu et al. (2019) studied extreme cold and drought in the Mongolian Plateau from 1969 to 2017 and found that despite the climate warming in the past 49 years, the frequency of cool days (TX10p) and cool nights (TN10p) in the Mongolian region has increased [12]. Kalita et al. (2023) conducted an analysis of significant changes in 21 extreme climate indices in Cherrapunji over the period from 1979 to 2020. Their study shows that indices related to daily maximum temperatures have significantly increased, while indices related to daily minimum temperatures have remained largely unchanged [16]. Therefore, understanding the characteristics and trends of extreme climate changes can help us better address the challenges and impacts brought by climate change.

Vegetation phenology is the study of how plants go through stages such as budburst, flowering, fruiting, and leaf fall under different seasonal and climatic conditions [17]. Vegetation phenology directly reflects how vegetation growth responds to environmental changes and has been garnering increasing attention in climate change research [14,18,19]. The SOS is a crucial phenological event in the growth process of vegetation. Variations in the SOS may modify vegetation activity, subsequently affecting the carbon cycle of ecosystems [20]. The SOS was closely associated with climate change [19,21], while the extent and direction of the SOS response to extreme climate events (such as drought and high temperatures) remain largely uncertain. Previous research has primarily focused on the impact of average climate change on the SOS [19,22–24]. Extreme climate changes have a more pronounced effect on the start of the growing season (SOS) compared to average climate variations [25,26]. For example, Piao et al. (2015) indicated that extreme temperature variations have a greater impact on the SOS in the Northern Hemisphere than average temperature changes [27]. Ma et al. (2015) reported that during a drought year, the SOS was delayed by 9.7 days, and during a wet year, the SOS was advanced by 25.8 days in Southeastern Australia, far exceeding the influence of average climate [26]. The response of the SOS to extreme climate events is highly complex and varies depending on both the type of event and the vegetation involved [10,28–30]. Ji et al. (2021) analyzed the response of the SOS to pre-season drought for various vegetation types in the North China Plain using GIMMS NDVI data from 1982 to 2015. The study found that pre-season drought leads to a delay in the SOS, with the most significant impact observed on the grassland SOS [28]. Studies have shown that extreme low-temperature events primarily drive the spring phenology in temperate China. The mean daily minimum temperature has the most significant impact on the mixed forest SOS, while the number of frost days has a greater effect on the grassland and sparse vegetation [10]. Therefore, it is essential to examine the response of the SOS to extreme climate events, especially in regions that are more vulnerable to climate change.

Mongolia, as a key region of the Mongolian Plateau, is situated within arid to semi-arid zones and ranks among the most sensitive areas to global climate change. In recent years, under the influence of global warming, the frequency and intensity of extreme climate events in Mongolia have been steadily increasing [9,31,32]. Previous studies have shown that between 2000 and 2010, the frequency of extreme drought and extreme cold events in the Mongolian Plateau increased steadily. Severe droughts occurred in 2001 and 2009, while an extreme cold event occurred in 2010 [31]. Many scholars have analyzed the SOS and its driving factors in the Mongolian Plateau [33–37]. Mei et al. (2021) analyzed the elevation dependence of spring phenology in the northwestern mountainous area of Mongolia and its impact on vegetation growth based on MODIS data from 2001 to 2018. They found that the SOS occurred earlier in low-elevation areas, and the spatiotemporal changes of the SOS were mainly affected by spring temperature and winter precipitation [35]. Based on GIMMS normalized difference vegetation index (NDVI) data from 1982 to 2015, Wu Rihan

et al. (2022) found that the sensitivity of the SOS in the Mongolian plateau grassland to pre-season drought was significantly reduced [33]. However, previous studies in Mongolia have primarily focused on spatiotemporal changes in the extreme climate indices and their effects on vegetation cover, with limited attention paid to the relationship between extreme events and the SOS [15,32,38]. To ensure the healthy development of livestock farming and to optimize pasture resource management, it is essential to accurately understand the response of diverse vegetation types' SOS to extreme climate change, further revealing their sensitivity to extreme climate indices. Compared to traditional studies that focus on the effects of average temperature or precipitation, this research introduces extreme climate indices to provide a more detailed analysis of the sensitivity of diverse vegetation types' SOS to extreme events. Therefore, this study first utilizes daily maximum, average, and minimum temperatures, as well as daily precipitation data from 1983 to 2016, to identify extreme drought, extreme heat, extreme cold, and extreme wet events during the period from 2000 to 2016. Next, it investigates the impact of extreme climate events on the spring phenology of diverse vegetation types in Mongolia and finally determines the sensitivity of the SOS of different vegetation types to extreme climate indices.

2. Materials and Methods

2.1. Study Area

Mongolia is located in Central Asia, bordered by China to the south and Russia to the north (41°35′ N to 52°09′ N, 87°44′ E to 119°56′ E). As a landlocked country, it encompasses a total land area of 1.564116 million square kilometers [39], making it the second-largest landlocked country in the world, following Kazakhstan. The terrain of Mongolia gradually decreases in elevation from west to east (see Figure 1a), with an average elevation of 1580 m. Being situated far from the ocean, Mongolia experiences a typical continental climate characterized by arid and semi-arid conditions [40]. The winters are long and severe, while the summers are short and dry, often accompanied by a dzud, a phenomenon that contributes to cold waves across the Eurasian continent. The average annual temperature ranges from −8 to 6 °C, and the average annual precipitation is relatively low, approximately 200 to 400 mm, with most of the rainfall concentrated in the summer months of June to August. The vegetation in Mongolia varies, transitioning from forest in the north to grassland and ultimately to sparse desert vegetation in the south [41,42].
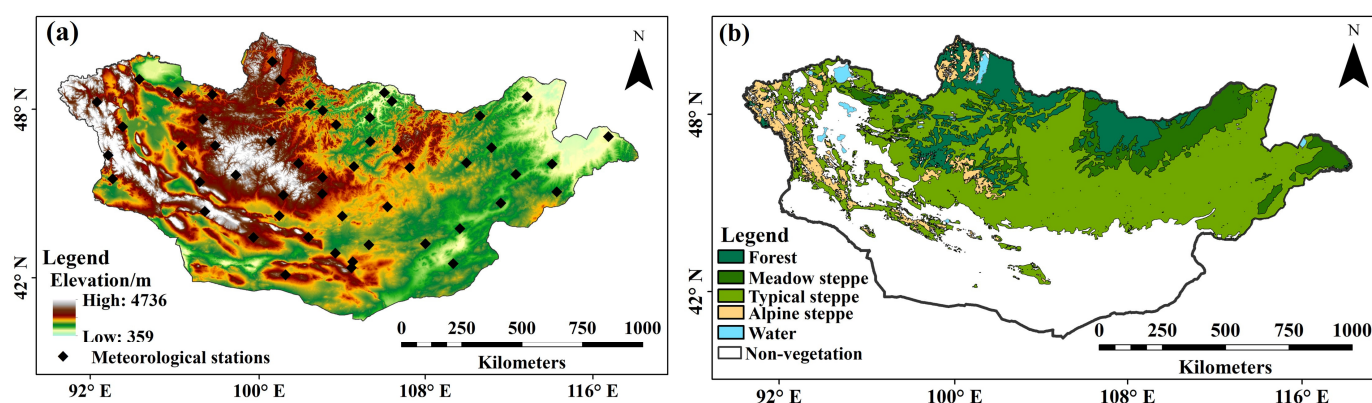
Figure 1. Location of Mongolia and spatial distribution of meteorological stations (**a**) and vegetation types (**b**).

2.2. Dataset

2.2.1. Extreme Climate Indices

This study utilized daily climate observation data from 53 meteorological stations throughout Mongolia, provided by the Institute of Geography and Geoecology at the Mongolian Academy of Sciences, covering the period from 1983 to 2016. The dataset includes daily maximum, mean, and minimum temperatures, as well as daily precipitation.

The RClimDex model was employed to conduct quality control analysis on the raw data and to calculate 10 extreme climate indices. These indices encompass eight extreme temperature indices and two extreme precipitation indices. Detailed information is presented in Table 1.

Table 1. Definitions of extreme climate indices.

Index	Indicator Name	Definition	Unit
TNn	Min Tmin	A monthly minimum of TN	°C
TNx	Max Tmin	A monthly maximum of TN	°C
TXn	Min Tmax	A monthly minimum of TX	°C
TXx	Max Tmax	A monthly maximum of TX	°C
TX10p	Cool days	Number of days when TX < 10th percentile	d
TX90p	Warm days	Number of days when TX > 90th percentile	d
TN10p	Cool nights	Number of days when TN < 10th percentile	d
TN90p	Warm nights	Number of days when TN > 90th percentile	d
RX1day	Maximum one-day precipitation	Highest precipitation amounts in 1 day	mm
RX5day	Maximum five-day precipitation	Highest precipitation amounts in 5 days	mm

TN and Tmin represent the minimum temperature; TX and Tmax represent the maximum temperature.

The data collected from each meteorological station are stored in a text format and organized by year, month, day, precipitation, maximum temperature, and minimum temperature, with the values separated by spaces. We compared records from neighboring stations by conducting a manual check and retained only the data that appeared reasonable. Any data identified as illogical or implausible were flagged as missing values and assigned a uniform value of −99.9. Upon completion of the quality control process, the data were prepared for calculations, resulting in a series of output files saved in Excel format. Taking into account the impact of pre-season temperature and precipitation on greening, the annual extreme climate indices are determined using data from October of the previous year to May of the current year. The extreme climate indices for all stations are then interpolated using Kriging to generate raster images with the same projection and pixel size as the NDVI data.

2.2.2. NDVI Data

NDVI datasets for the study area were obtained from the MOD13A2 product, covering the years 2001 to 2016, with a temporal resolution of 16 days and a spatial resolution of 1 km (https://search.earthdata.nasa.gov, accessed on 13 June 2023). To minimize the impact of clouds, solar elevation angle, and atmospheric conditions on the raw data, we employed harmonic analysis of NDVI time series to smooth and reconstruct the 23 composite NDVI scenes synthesized on an annual basis. Furthermore, to mitigate the influence of areas characterized by minimal vegetation cover on the study outcomes, regions with an average NDVI below 0.08 over multiple years were identified as non-vegetated areas and subsequently excluded from the analysis.

2.2.3. Vegetation Types

The vegetation type data were sourced from the *National Atlas of Mongolia*. The vegetation data from the atlas underwent processes such as scanning, geometric correction, and digitization. As a result, four vegetation types were identified: forest, meadow steppe, typical steppe, and alpine grassland (Figure 1b). These categories were used to analyze the start of the growing season (SOS) for different vegetation types and their sensitivity to extreme climate indices.

2.3. Methods

2.3.1. Explanation of Extreme Climate Events

Extreme climate events refer to weather phenomena characterized by significant deviation in climate variables (such as temperature, precipitation, wind speed, etc.) from the normal range for a specific region and time period [43,44]. These events are often of

extremely high intensity and can have substantial impacts on the environment, society, and economy. This study investigates extreme climate events that occurred in Mongolia from 2000 to 2016, focusing on extreme warm, extreme wet, extreme dry, and extreme cold events. Prior to calculating temperature and precipitation anomalies, based on daily temperature and precipitation data from each meteorological station from 1983 to 2016, we considered the influence of pre-season precipitation and temperature on green-up. We used data from 1 September of the previous year to 31 August of the current year to obtain each year's mean temperature and total precipitation, ultimately deriving the multi-year average temperature and precipitation. The annual climate anomalies for all 53 meteorological stations within the study area were calculated using Formula (1), and observations were defined as extreme events when anomaly changes exceeded the 75th and 25th percentiles [25]:

$$A_j = \frac{\sum X_{i,j} - \overline{X}_i}{n} \tag{1}$$

where A_j represents the climate anomaly for year j; $X_{i,j}$ represents the temperature/precipitation for station i in year j; $\overline{X}_i$ represents the average temperature/precipitation for station *i* from 1983 to 2016; and n is the total number of stations. Based on the annual anomaly variations in temperature and precipitation, the criteria shown in Table 2 are employed to identify the following extreme situations: (1) Extreme dry events: the temperature is as close to the average as possible, but precipitation is below the 25th percentile anomaly reference line. (2) Extreme warm events: the temperature exceeds the 75th percentile anomaly reference line, with precipitation remaining close to the average. (3) Extreme cold events: the temperature is below the 25th percentile anomaly reference line, while precipitation is as close to the average as possible. (4) Extreme wet events: the temperature is near the average, but precipitation exceeds the 75th percentile anomaly reference line.

Table 2. Climatic observations that fell outside the 25th and 75th percentiles of the yearly anomaly time series were identified as extremes.

Extreme Climate Event	Tmax	Tmean	Tmin	P
Extreme dry event	$A_j \to 0$	$A_j \to 0$	$A_j \to 0$	$A_j < 25\%$
Extreme warm event	$A_j > 75\%$	$A_j > 75\%$	$A_j > 75\%$	$A_j \to 0$
Extreme cold event	$A_j < 25\%$	$A_j < 25\%$	$A_j < 25\%$	$A_j \to 0$
Extreme wet event	$A_j \to 0$	$A_j \to 0$	$A_j \to 0$	$A_j > 75\%$
Normal year	$A_j \to 0$	$A_j \to 0$	$A_j \to 0$	$A_j \to 0$

Tmax represents maximum temperature; Tmean represents maximum temperature; Tmin represents minimum temperature; P represents precipitation; A_j represents climate anomaly for year *j*.

2.3.2. SOS Extraction

The smoothed and reconstructed NDVI data were used to identify the SOS at the pixel scale using the cumulative NDVI-based logistic curvature method [45]. The cumulative NDVI-based logistic curvature method is based on the annual cumulative NDVI. It involves fitting the cumulative NDVI with a logistic function (22), calculating the curvature of the fitted curve using Formulas (3) and (4), and defining the time corresponding to the maximum curvature as the SOS.

$$y(t) = \frac{c}{1 + e^{a+bt}} + d \tag{2}$$

where *y(t)* represents the cumulative NDVI value fitted with a logistic function corresponding to Julian day *t*; d is the background NDVI; *c + d* is the maximum cumulative NDVI

value; and a and b are the fitting parameters. The curvature of the fitted curve is calculated using Formulas (3) and (4):

$$k = \frac{d\alpha}{ds} = \frac{b^2 cz(1-z)(1+z)^3}{\left[(1+z)^4 + (bcz)^2\right]^{1.5}}$$

(3)

$$z = e^{a+bt}$$

(4)

where k represents the curvature of the cumulative NDVI Logistic fitting curve; α represents the angle of the unit tangent vector; s is the unit length along the fitted curve; and z is the parameter.

2.3.3. Statistical Analysis
Radial Basis Function (RBF)

Using the variable importance of the RBF neural network model, we ranked the impact of 10 extreme climate indices on the SOS for different vegetation types. In this study, the RBF neural network was used as the analysis tool. The 10 extreme climate indices affecting the SOS—TXn, TXx, TNn, TNx, TX10p, TX90p, TN10p, TN90p, RX1day, and RX5day—were all input into the RBF neural network's input layer, with the SOS as the output layer. By simulating the effect of extreme climate indices on the SOS, we ranked the indices based on their influence on the vegetation SOS. This ranking facilitated a detailed analysis of how various vegetation types respond to different extreme climate indices.

Sensitivity of the SOS to Extreme Climate Indices

The sensitivity of the SOS to extreme climate indices was analyzed using the multiple linear regression method. We set the SOS as the dependent variable, and the extreme climate indices were set as the independent variables. The sensitivity of the SOS for different vegetation types to extreme climate indices was calculated on a per-pixel basis using a multiple linear regression method. In this analysis, the regression coefficient (slope) represents the degree of sensitivity.

$$Y = \beta_0 + \beta_1 X_1 + \beta_2 X_2 + \cdots + \beta_k X_k + \mu$$

(5)

where β_0 represents a constant, and μ represents random error. y represents the SOS data for the years 2001, 2007, 2010, and 2013; $X_1, X_2, \ldots X_k$ represent the extreme climate indices with greater importance for the years 2001, 2007, 2010, and 2013, respectively; and $\beta_1, \beta_2, \cdots, \beta_k$ represent multiple linear regression coefficients, indicating the sensitivity characteristics of the SOS to extreme climate indices.

3. Results

3.1. Extreme Climate Events in Mongolia

According to meteorological data from 1983 to 2016, the variations of temperature and precipitation anomalies are depicted in Figure 2. The data showed that the maximum, average, and minimum temperatures in the study area increased at rates of 0.39 °C, 0.37 °C, and 0.27 °C per decade, respectively (Figure 2a–c), indicating a significant warming trend across Mongolia ($p < 0.05$). Among them, the rate of increase in maximum temperature was 1.4 times that of minimum temperature. The annual precipitation anomaly curve (Figure 2d) shows that Mongolia's annual precipitation decreased at a rate of 5.95 mm per decade from 1983 to 2016, although this decreasing trend was not significant ($p = 0.12$). However, between 2004 and 2010, annual precipitation was lower than the long-term average. Over the past few decades, temperatures have increased significantly, with a rise in the frequency of high-temperature events, while the frequency of cold events has decreased. In recent years, especially since 2000, significant warming has been dominant. Between 1983 and 1999, cold events mainly occurred in 1983, 1984, 1985, 1987, and 1988,

while high-temperature events only occurred twice, in 1997 and 1998. However, since 2000, the frequency of high-temperature events has increased significantly, occurring five times in 2002, 2007, 2009, 2014, and 2015. Based on these characteristics of climate change in Mongolia, four extreme climate events were identified: extreme drought in 2001, extreme high temperature in 2007, extreme cold in 2010, and extreme wet conditions in 2013.
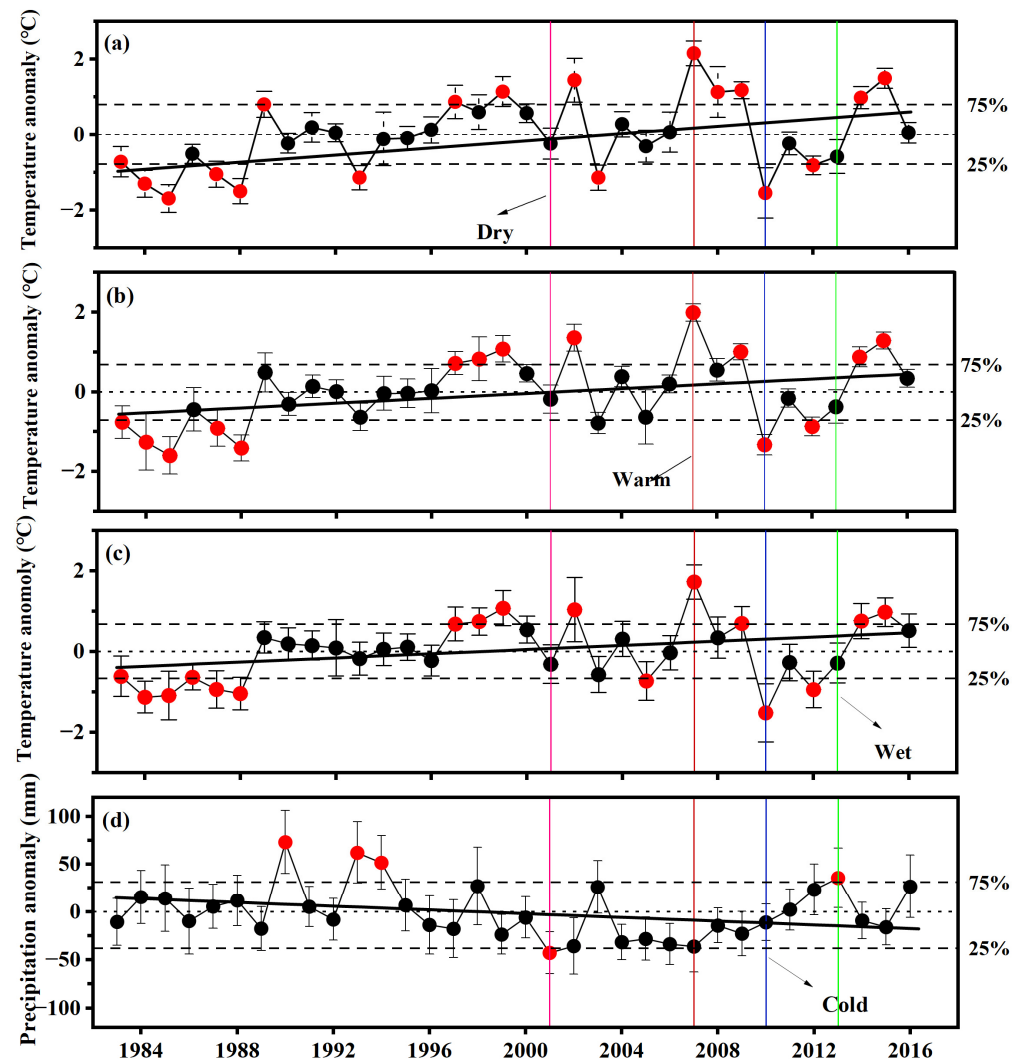

Figure 2. Plotted mean climatological departures of Mongolia from 1983 to 2016 for (**a**) maximum temperature, (**b**) mean temperature, (**c**) minimum temperature, and (**d**) precipitation. The pink, red, blue, and green lines correspond to extremely dry, warm, cold, and wet years, respectively. The red and black circles represent extreme and normal values of climate observations, respectively.

3.2. Spring Phenological Response to Extreme Climate Events

SOS anomalies refer to the deviation of the SOS relative to the long-term average. In other words, the anomaly represents the difference between the SOS of a specific year or period and the multi-year average SOS. Positive anomalies indicate a delayed SOS (i.e., the start of plant growth occurs later than the average), while negative anomalies indicate an earlier SOS (i.e., the start of plant growth occurs earlier than the average). Figure 3a–d illustrates the spatial distribution patterns of the SOS anomalies relative to the long-term average for the four most extreme years (2001, 2007, 2010, and 2013) within the period from 2001 to 2016. In 2001, 62.8% of the pixels across Mongolia showed an advancement in the SOS, mainly distributed throughout the Khangai Mountains region, while the eastern side of the Khentii Mountains experienced a delay in the SOS (Figure 3a,e). Based on Figure 3b,f, extreme warmth led to an advancement in the SOS in 79.0% of the study

area, primarily concentrated in the western Khangai Mountains and the eastern Dornod Province. Conversely, extreme cold resulted in a delay in the SOS for 57.9% of the study area, mainly situated on the eastern side of the Khentii Mountains in Khentii Province and Dornogovi Province (Figure 3c,g). The areas showing advancement in the SOS were almost equal in proportion to those exhibiting delays, accounting for 53.1% and 43.1% of the total pixels, respectively. Areas showing advancement were predominantly located in the southwestern part of the study area and the southern part of the Khangai Mountains, while areas exhibiting a delay were mainly distributed on the eastern side of the Khentii Mountains (Figure 3d,h).
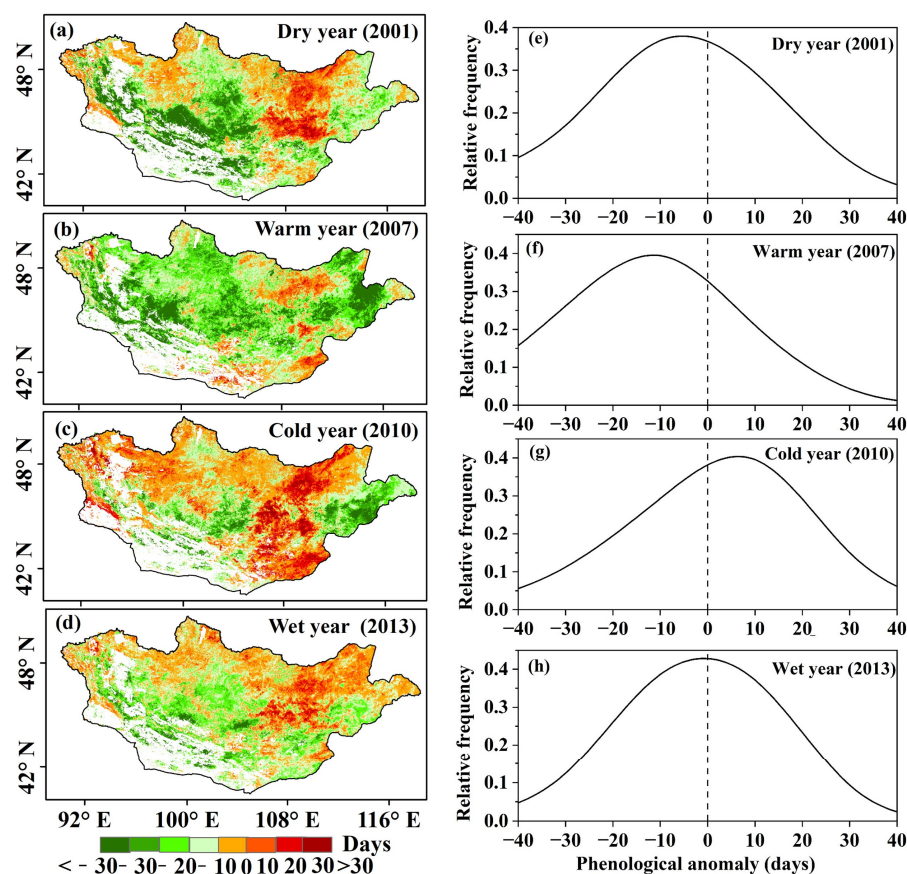

Figure 3. Spatial distribution of SOS anomalies on extreme climate events (**a**–**d**). Plot of the relative frequency of SOS anomalies for extreme climate events (**e**–**h**).

Figure 4 illustrates the changes in the average SOS anomalies across the entire study area in Mongolia and among different vegetation types during extreme climate events. As shown in Figure 4a, during the extreme drought year, the SOS across the entire study area in Mongolia was advanced by 6.9 days (ΔSOS = −6.9 days) compared to the 17-year average SOS from 2001 to 2016. In the extreme wet year, the SOS in the entire study area exhibited a slight average advancement of 1.2 days (ΔSOS = 1.2 days). In warm years, there was an advancement in the SOS, with an average advance of 13.2 days (ΔSOS = −13.2 days), while in cold years, there was an average delay of 1.2 days (ΔSOS = 1.2 days). Diverse vegetation types respond differently to extreme climate events (Figure 4b). Forest had the least responsive SOS to extreme dryness and wetness, with a change of only 0.3 days and 1.08 days (ΔSOS = 0.3 days and ΔSOS = 1.1 days). The SOS in alpine steppes shows the greatest change during extreme drought and extreme heat events, leading to an earlier SOS, with advances of 8.3 and 15.5 days, respectively (ΔSOS = −8.3 days and ΔSOS = −15.5 days). Regarding extreme warm conditions, typical steppes had the greatest change on the SOS, advancing it by 17.2 days (ΔSOS = −17.2 days). However, extreme cold conditions had the

most significant effect on meadow steppes, delaying the SOS by 6.8 days (ΔSOS = 6.8 days). Overall, the response of the SOS to extreme warm conditions is more pronounced across various vegetation types compared to other extreme events.
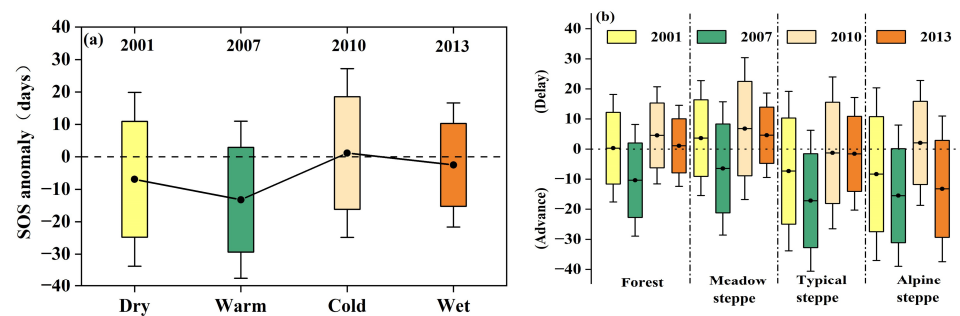

Figure 4. (**a**) The changes in the average SOS anomalies (black point) across the entire study area in Mongolia. (**b**) SOS anomalies among the four vegetation types during extreme climate events.

3.3. The Importance of Extreme Climate Indices on the Phenology of Diverse Vegetation Types

The RBF model was utilized to evaluate the impact of 10 extreme climate indices (Table 1) on the SOS for various vegetation types in Mongolia during extreme climate events. Higher values indicate a greater importance of the variable. As shown in Figure 5, specific attention is paid to the responses of forest, meadow steppe, typical steppe, alpine grassland, and the overall region's SOS to these extreme climate indices.

The importance of different extreme climate indices at the SOS for various vegetation types is illustrated in Figure 5a–e. For extremely dry years, it is evident that the SOS of forest vegetation is primarily influenced by the RX5day, RX1day, TN10p, and TX90p indices. The meadow steppe SOS is affected by the RX5day, RX1day, TN90p, and TNx indices. The typical steppe SOS is significantly influenced by extreme temperature indices, primarily the TNx, TXn, TN90p, and TX90p indices. The SOS of the alpine steppe is predominantly affected by the TX10p, RX5day, TXn, and RX1day indices. The overall regional SOS is strongly influenced by the RX5day, RX1day, TXn, and TN90p indices.

In extremely warm years, depicted in Figure 5f–j, the forest SOS is mainly affected by the RX5day, RX1day, TX10p, and TN10p indices. The meadow steppe SOS is significantly impacted by the TXx, TXn, TX10p, and RX1day indices, while the typical steppe SOS is primarily influenced by the TN10p, RX5day, TX10p, and TXn indices. The alpine steppe SOS is mainly driven by the TX10p, TN10p, TNx, and TXx indices. Overall, the regional SOS is most strongly influenced by the TXn, RX1day, RX5day, and TX10p indices.

For extreme cold events, as shown in Figure 5k–o, the forest SOS is primarily influenced by the TXx, TX90p, TN10p, and RX1day indices. The meadow steppe SOS is affected by the TX90p, RX1day, TNx, and TN90p indices. The SOS of the typical steppe is mainly influenced by the TXn, TNn, TNx, and TN90p indices, while the alpine steppe SOS is driven by the TNx, RX1day, RX5day, and TX90p indices. The overall regional SOS is predominantly influenced by the TXn, TNn, TX90p, and TNx indices, with extreme temperature indices having a significant impact on the entire region.

For extreme wet events, as depicted in Figure 5p–t, the forest SOS is mainly influenced by the TN90p, RX5day, TX90p, and RX1day indices. The meadow steppe SOS is primarily affected by the TX90p, TX10p, RX1day, and TN90p indices. The typical steppe SOS is most influenced by the TNx, TXn, RX1day, and TN10p indices. The alpine steppe SOS is driven by the TX10p, TN10p, RX5day, and TNn indices. Overall, the regional SOS is primarily influenced by the TXn, TNx, TX10p, and TXx indices, with extreme temperature indices having a notable impact across the region.

Based on the impact of the 10 extreme climate indices on the SOS across the entire study area and diverse vegetation types, we selected four key extreme climate indices to analyze the sensitivity of the SOS to each extreme climate event. The selected indices for an extreme dry year were RX5day, RX1day, TXn, and TN90p. For an extremely warm year, the

selected indices were RX5day, RX1day, TXn, and TX10p. For an extremely cold year, the selected indices were TNn, TNx, TXn, and TX90p. Finally, for an extremely wet year, the selected indices were RX5day, TXn, TNx, and TX10p.
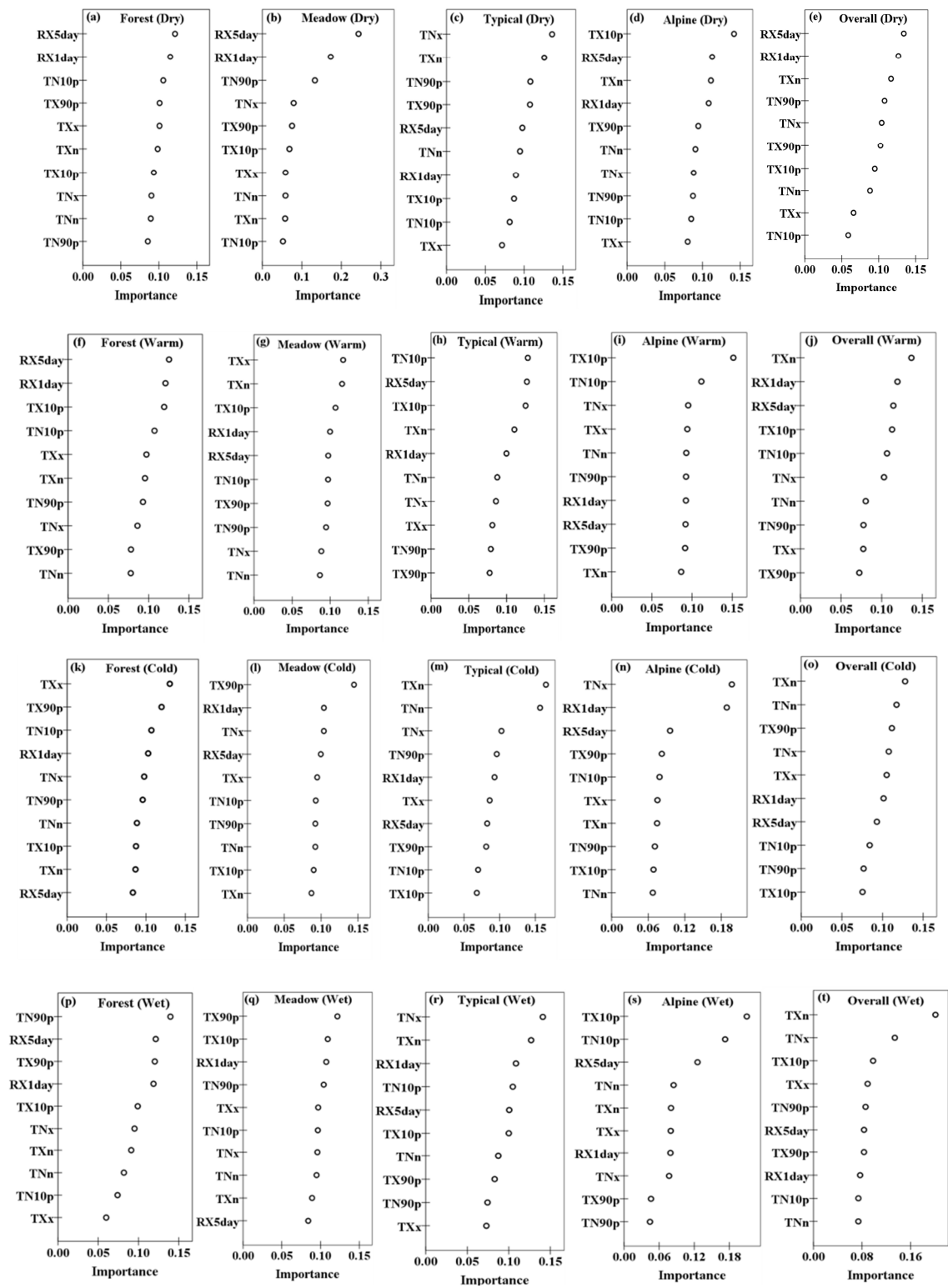

Figure 5. The importance of 10 extreme climate indices to the diverse vegetation types of spring phenology is shown in each year of extreme climate events: (**a–e**) extremely dry; (**f–j**) extremely warm; (**k–o**) extremely cold; and (**p–t**) extremely wet years.

3.4. Sensitivity of Spring Phenology to Extreme Climate Indices

Analyzing the sensitivity of SOS across the entire study area and for different vegetation types to extreme climate indices in the context of four extreme climate events will help deepen the understanding of how SOS responds to extreme climate indices. The sensitivity of SOS to extreme climate indices further illustrates its response to pre-season precipitation and pre-season temperature. This analysis will have important implications for ecosystem stability and adaptation planning.

As shown in Figure 6a, under extreme drought conditions, the SOS for the entire study area, meadow steppe, and typical steppe exhibits the strongest sensitivity to the TN90p index, with sensitivity coefficients of −2.91, −2.95, and −3.01, respectively. These significant negative sensitivities indicate that the SOS in these regions is more sensitive to temperature than to precipitation. The increase in the number of warm nights leads to an earlier SOS in these areas. Conversely, the SOS for forests and alpine steppe shows the highest sensitivity to the RX1day index, with sensitivity coefficients of −3.37 and −3.31, respectively. This significant negative sensitivity indicates that the SOS in forests and alpine steppe are more sensitive to precipitation than to temperature. An increase of one day of precipitation results in an earlier SOS for these ecosystems. As shown in Figure 6b, during an extreme warm event, the SOS for the entire study area exhibits the strongest negative sensitivity to the TX10p; the sensitivity coefficient is −7.54, indicating that an increase in cool days leads to an earlier SOS. Among them, the SOS of the meadow steppe is the most sensitive to the TX10p, with a sensitivity coefficient of 15.87, while the SOS for typical steppe shows the weakest sensitivity, with a coefficient of −6.09. The SOS of forests and meadow steppe are positively correlated with the TX10p, whereas the typical steppe and alpine steppe show a negative correlation.
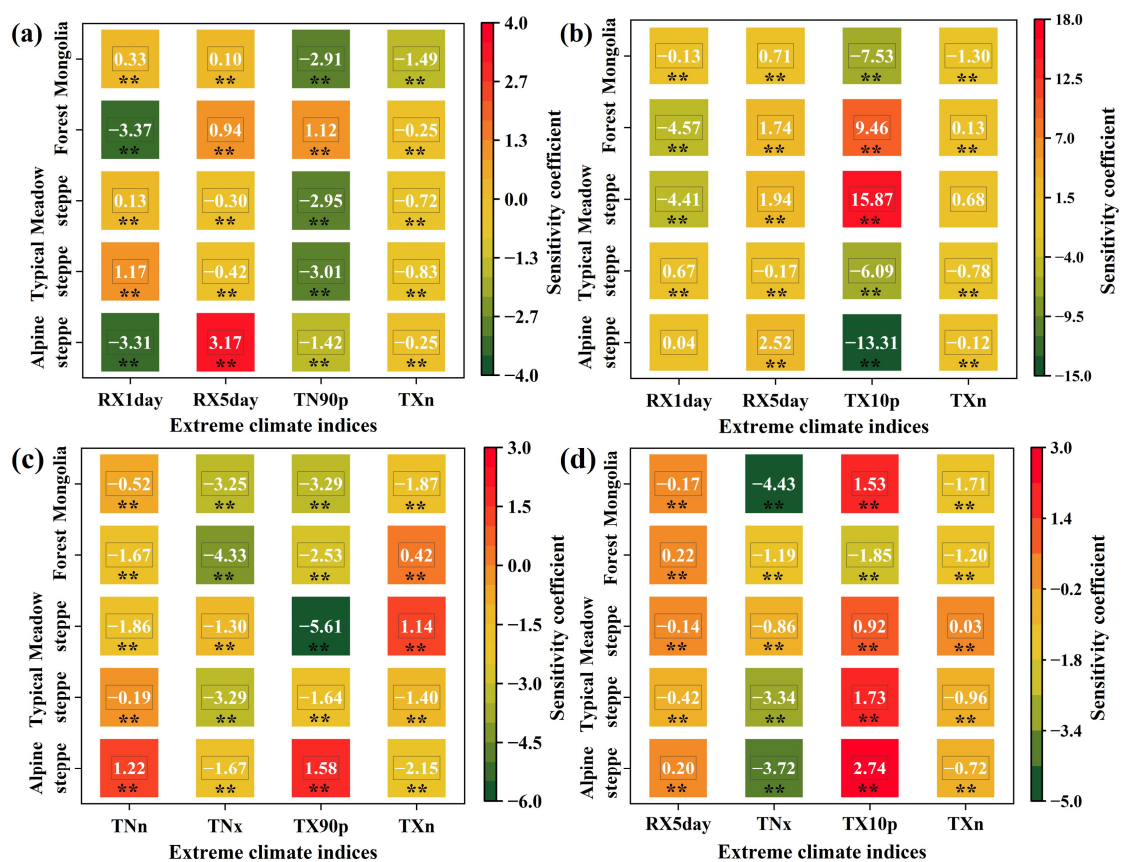

Figure 6. The sensitivity of four extreme climate indices to the entire study area and diverse vegetation types of spring phenology is shown in each year of extreme climate events: (**a**) extreme dry, (**b**) extreme warm, (**c**) extreme cold, and (**d**) extreme wet years. ** represents 0.01 significance level.

During the extreme cold year, the SOS for the entire study area and diverse vegetation types are most significantly affected by extreme temperature indices (Figure 6c). The SOS of forests and typical steppe are highly responsive to the TNx; the sensitivity coefficients are −4.33 and −3.29, resulting in a significant negative sensitivity. This means that an increase in TNx leads to an earlier SOS for forests and typical steppe. The entire study area and meadow steppe SOS are most sensitive to the TX90p; the sensitivity coefficients are −3.29 and −5.61, while alpine steppe is most sensitive to the TXn; the sensitivity coefficient is −2.15. This indicates that an increase in TX90p leads to an earlier SOS for meadow steppe, and an increase in TXn leads to an earlier SOS for alpine steppe. As shown in Figure 6d, during extreme wet conditions, the SOS of forests and meadow steppe are most affected by the TX10p; the sensitivity coefficients are −1.85 and 0.92, emphasizing the impact of cool days on the SOS of these vegetation types. The forest SOS exhibits negative sensitivity to TX10p, while the meadow steppe SOS shows positive sensitivity to TX10p. The SOS of the entirety of Mongolia and typical steppe and alpine steppe are most sensitive to the TNx, resulting in negative sensitivity; the sensitivity coefficients are −4.33, −3.34, and −3.72, respectively. This suggests that an increase in TNx leads to an earlier SOS for both typical and alpine steppes.

4. Discussion

The start of the growing season (SOS) serves as an important indicator of climate warming and is particularly sensitive to temperature changes [46]. Before spring green-up, vegetation undergoes two temperature-driven dormancy stages: endodormancy and ecodormancy. During endodormancy, plants require a period of low-temperature chilling to break dormancy, highlighting the key role of low temperatures in plant growth. Once this chilling requirement is met, vegetation enters ecodormancy, where it begins to accumulate heat. When a critical heat threshold is reached, vegetation finally initiates green-up [47]. The increasing intensity and frequency of extreme climate events adds uncertainty to predictions of climate change's effects on ecosystems [8,10,26]. Thus, it is urgent to study how terrestrial ecosystems respond to the increasingly severe extreme climate events.

Research has indicated that Mongolia is experiencing a more significant rise in its maximum daily temperatures compared to its minimum daily temperatures. The rate of warming for the maximum daily temperature is outpacing that of the minimum daily temperature, resulting in an expansion of the diurnal temperature range. This pattern deviates from the trend observed in most other regions worldwide, where the increase in the minimum daily temperatures exceeds that of the maximum temperature [48,49].

In Mongolia, extreme dryness has caused the SOS to occur earlier compared to the multi-year average SOS from 2001 to 2016, which is contrary to the findings of many previous studies. The results of this study are consistent with [50], which found that, in the Northern Hemisphere, the SOS in years of extreme pre-season drought occurred an average of 1.9 days earlier than in normal years and 3.7 days earlier than in wet years. The SOS of the Mongolian Plateau steppe tends to advance in normal years, while in drought years, the SOS is delayed [33], which is consistent with the delayed SOS observed in the meadow steppe in this study. Ge et al. found that the extreme dryness of 2010 delayed the SOS on the YunGui Plateau, Southwest China, by 10.8 days [51]. There may be two reasons for the results observed in this study. First, the water limitations caused by drought may not offset the impact of temperature on the SOS. Our findings indicate that under extreme drought conditions, the sensitivity of SOS to extreme temperature indices in both meadows and typical steppes across the entire study area is greater than its sensitivity to extreme precipitation indices (Figure 6a). Furthermore, the correlation analysis between SOS and monthly precipitation and temperature from October of the previous year to May of the current year (Figure 7a) further highlights the crucial role that pre-season temperature plays in influencing SOS. At the same time, Mongolia is located in arid and semi-arid regions, where vegetation typically exhibits strong drought resistance [52] and high resilience to drought stress [53], allowing it to adapt to water-scarce environments. Second, under

extreme drought conditions, as spring temperatures gradually rise, the melting of snow or frozen soil replenishes soil moisture, which in turn alleviates drought stress [54]. As shown in Figure 7a, the correlation between precipitation from October to January of the previous year and the SOS is higher than that of other months. The relative stability of the SOS of the forest compared to other vegetation types may be attributed to the deep root systems and higher water-use efficiency of forests. These characteristics allow forests to better utilize soil water resources under extremely dry conditions [55,56]. The delay in the SOS for meadow steppes could be attributed to a higher nighttime temperature, which hinders the fulfillment of chilling requirements and prolongs the dormancy period [57]. Given that precipitation is the primary driver of vegetation changes in alpine steppes [44], it is highly likely that it accounts for the heightened sensitivity of the alpine steppe SOS to RX1day during extreme dryness events.
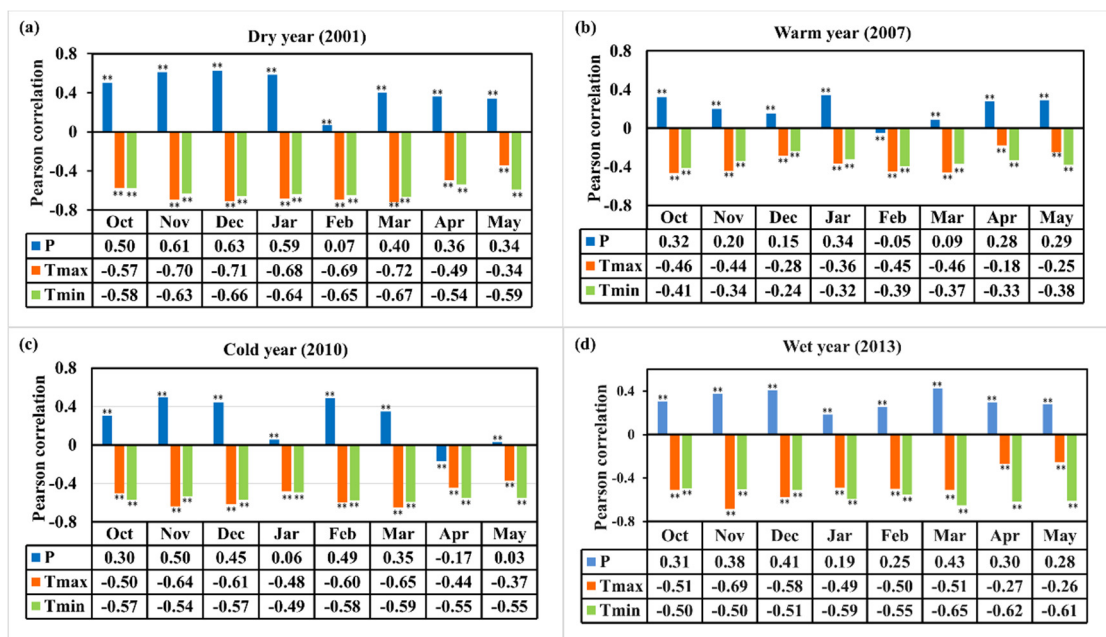

Figure 7. The correlation of the SOS with precipitation and temperature across the entire study area during extreme climate events (**a**–**d**). ** represents 0.01 significance level.

The extreme wetness event in 2013 led to an overall advancement in the SOS in the study area, consistent with the results of Li et al. (2021) [22]. The main reason for this result is that under conditions of sufficient precipitation, vegetation spring phenology is primarily driven by temperature [58]. The greater sensitivity of the SOS to extreme temperature indices compared to extreme precipitation indices further indicates that under extremely wet conditions, temperature has a more significant impact on spring phenology than precipitation (Figure 7d). The advancement of SOS in typical steppe and alpine meadow can be mainly attributed to the influence of nighttime temperatures on vegetation growth in these areas. The warming of nighttime temperatures may enhance the frost resistance of vegetation [59], consequently reducing the risk of frost damage [60].

The extremely warm year in 2007 led to an overall advancement in the SOS in Mongolia, consistent with findings from other studies [25,61]. While all vegetation types experienced an advancement in the SOS, the extent of this advancement varied. This may be attributed to rising temperatures effectively meeting the heat accumulation required for vegetation green-up [62]. Additionally, increased temperatures lead to snowmelt, which in turn enhances soil moisture [63], and provides favorable environmental conditions for vegetation green-up. The sensitivity of SOS across vegetation types to the TX10p index is the highest, further indicating that daytime temperatures have a greater impact on vegetation SOS. Among these, typical steppe exhibits the most significant advancement in SOS

compared to other vegetation types, likely due to the low precipitation and arid climate of typical steppe regions [25], which result in heat-resistant vegetation. Additionally, the dominant grasses in these areas have shallow, well-developed root systems that can rapidly absorb available water [64]. During periods of extreme heat, soil moisture from melting snow may further support the growth of typical steppe vegetation. Conversely, the extreme cold event in 2010 resulted in an overall delay in the SOS in Mongolia, consistent with other research findings [10]. Extreme temperature indices have a profound effect on the SOS. The sensitivity of the SOS to extreme temperature indices is the highest. The meadow and alpine steppe SOS respond most strongly to daytime temperatures, likely because lower daytime temperatures slow the accumulation of heat required for vegetation germination and leaf emergence [62]. In contrast, the SOS for forests responds most strongly to nighttime temperatures, suggesting that lower nighttime temperatures may increase the risk of frost damage. To mitigate frost injury, vegetation delays its green-up [65]. The minimal change in the SOS in alpine steppe may be due to their high-altitude location, where temperatures remain relatively low. Under extreme cold conditions, alpine steppe has a strong adaptation to low temperatures [66], which contributes to the stability of its SOS.

Compound extreme climate events can involve multiple climate factors occurring simultaneously or sequentially, such as extreme drought combined with high temperatures or severe storms followed by heavy rainfall. These complex climatic conditions can place greater stress on vegetation, affecting its growth and physiological processes. For instance, Choukri et al. (2020) found that lentils had a mean flowering time of 69 days under normal sowing conditions, whereas under compound high temperature and drought stress, the mean flowering time was reduced to 44 days, indicating that compound drought and a warm event significantly shorten the flowering time of lentils [67]. The impact of compound extreme climate events on vegetation phenology is a topic of significant concern. While past research has acknowledged the effects of individual extreme climate events on vegetation phenology, studies on the impact of compound extreme climate events are relatively scarce. Since these events can have more complex and extensive effects [25,68], it is crucial to conduct in-depth research on how vegetation phenology responds to them.

5. Conclusions

Extreme climate events significantly impact the start of growing season (SOS) for different vegetation types in Mongolia. Investigating the effects of these events on the growing cycles of Mongolian vegetation is essential for several reasons: it aids in evaluating and forecasting future phenological dynamics, forming effective environmental management and climate adaptation strategies, and deepening our understanding of the carbon and water cycles in terrestrial ecosystems. This study utilizes MODIS NDVI data from 2001 to 2016, along with data from 53 Mongolian meteorological stations spanning from 1983 to 2016. These stations provide daily maximum, mean, and minimum temperatures, as well as daily precipitation levels. By examining defined extreme climate events, the study analyzes the SOS variations across different vegetation types and their sensitivity to pre-season extreme climate indices, leading to the following conclusions:

(1) From 1983 to 2016, Mongolia experienced a significant warming trend, with pre-season maximum temperatures rising at a rate 1.4 times faster than minimum temperatures. Precipitation displayed a non-significant decreasing trend. Specific years were identified as extreme climate event years: 2001 as an extreme dry year, 2007 as an extremely warm year, 2010 as an extremely cold year, and 2013 as an extremely wet year.

(2) The SOS in Mongolia responds differently to extreme climate events. Extreme drought, warm, and wet events tend to trigger an earlier SOS compared to the multi-year average SOS from 2001 to 2016, while extreme cold events result in a delayed SOS. Furthermore, the response of the SOS to extreme climate events varies among different vegetation types.

(3) During extreme climate events, the sensitivity of the SOS in Mongolia to extreme climate indices varies. In extreme drought and wet events, minimum temperature is

the primary driver of SOS, whereas maximum temperature plays a key role in extreme warm and cold events. The sensitivity of the SOS to these climate indices also differs among diverse vegetation types.

References

1. Masson-Delmotte, V.; Zhai, P.; Pirani, S.; Connors, C.; Péan, S.; Berger, N.; Caud, Y.; Chen, L.; Goldfarb, M.; Scheel Monteiro, P.M. Summary for policymakers. In *Climate Change 2021: The Physical Science Basis. Contribution of Working Group i to the Sixth Assessment Report of the Intergovernmental Panel on Climate Change*; IPCC: Geneva, Switzerland, 2021. Available online: https://www.ipcc.ch/report/ar6/wg1/downloads/report/IPCC_AR6_WGI_SPM_final.pdf (accessed on 11 November 2024).
2. Coumou, D.; Rahmstorf, S. A decade of weather extremes. *Nat. Clim. Chang.* **2012**, *2*, 491–496. [CrossRef]
3. Easterling, D.R.; Meehl, G.A.; Parmesan, C.; Changnon, S.A.; Karl, T.R.; Mearns, L.O. Climate extremes: Observations, modeling, and impacts. *Science* **2000**, *289*, 2068–2074. [CrossRef]
4. Fernández-Giménez, M.E.; Batkhishig, B.; Batbuyan, B. Cross-boundary and cross-level dynamics increase vulnerability to severe winter disasters (dzud) in Mongolia. *Glob. Environ. Chang.* **2012**, *22*, 836–851. [CrossRef]
5. Xie, Y.; Wang, X.; Silander, J.A., Jr. Deciduous forest responses to temperature, precipitation, and drought imply complex climate change impacts. *Proc. Natl. Acad. Sci. USA* **2015**, *112*, 13585–13590. [CrossRef]
6. Camuffo, D.; della Valle, A.; Becherini, F. A critical analysis of the definitions of climate and hydrological extreme events. *Quat. Int.* **2020**, *538*, 5–13. [CrossRef]
7. Ciais, P.; Reichstein, M.; Viovy, N.; Granier, A.; Ogee, J.; Allard, V.; Aubinet, M.; Buchmann, N.; Bernhofer, C.; Carrara, A.; et al. Europe-wide reduction in primary productivity caused by the heat and drought in 2003. *Nature* **2005**, *437*, 529–533. [CrossRef]
8. Xu, C.; McDowell, N.G.; Fisher, R.A.; Wei, L.; Sevanto, S.; Christoffersen, B.O.; Weng, E.; Middleton, R.S. Increasing impacts of extreme droughts on vegetation productivity under climate change. *Nat. Clim. Chang.* **2019**, *9*, 948–953. [CrossRef]
9. Dashkhuu, D.; Kim, J.P.; Chun, J.A.; Lee, W.-S. Long-term trends in daily temperature extremes over Mongolia. *Weather Clim. Extrem.* **2015**, *8*, 26–33. [CrossRef]
10. Mo, Y.; Zhang, X.; Liu, Z.; Zhang, J.; Hao, F.; Fu, Y. Effects of Climate Extremes on Spring Phenology of Temperate Vegetation in China. *Remote Sens.* **2023**, *15*, 686. [CrossRef]
11. Li, Y.; Zhao, J.; Miao, R.; Huang, Y.; Fan, X.; Liu, X.; Wang, X.; Wang, Y.; Shen, Y. Analysis of the Temporal and Spatial Distribution of Extreme Climate Indices in Central China. *Sustainability* **2022**, *14*, 2329. [CrossRef]
12. Liu, Z.; Yao, Z.; Huang, H.; Batjav, B.; Wang, R. Evaluation of Extreme Cold and Drought over the Mongolian Plateau. *Water* **2019**, *11*, 74. [CrossRef]
13. Chen, K.; Ge, G.; Bao, G.; Bai, L.; Tong, S.; Bao, Y.; Chao, L. Impact of Extreme Climate on the NDVI of Different Steppe Areas in Inner Mongolia, China. *Remote Sens.* **2022**, *14*, 1530. [CrossRef]

14. Ying, H.; Zhang, H.; Zhao, J.; Shan, Y.; Zhang, Z.; Guo, X.; Rihan, W.; Deng, G. Effects of spring and summer extreme climate events on the autumn phenology of different vegetation types of Inner Mongolia, China, from 1982 to 2015. *Ecol. Indic.* **2020**, *111*, 105974. [CrossRef]

15. Ren, J.; Tong, S.; Ying, H.; Mei, L.; Bao, Y. Historical and Future Changes in Extreme Climate Events and Their Effects on Vegetation on the Mongolian Plateau. *Remote Sens.* **2022**, *14*, 4642. [CrossRef]

16. Kalita, R.; Kalita, D.; Saxena, A. Trends in extreme climate indices in Cherrapunji for the period 1979 to 2020. *J. Earth Syst. Sci.* **2023**, *132*, 74. [CrossRef]

17. Cleland, E.E.; Chuine, I.; Menzel, A.; Mooney, H.A.; Schwartz, M.D. Shifting plant phenology in response to global change. *Trends Ecol. Evol.* **2007**, *22*, 357–365. [CrossRef] [PubMed]

18. Pei, T.; Ji, Z.; Chen, Y.; Wu, H.; Hou, Q.; Qin, G.; Xie, B. The Sensitivity of Vegetation Phenology to Extreme Climate Indices in the Loess Plateau, China. *Sustainability* **2021**, *13*, 7623. [CrossRef]

19. Miao, L.; Muller, D.; Cui, X.; Ma, M. Changes in vegetation phenology on the Mongolian Plateau and their climatic determinants. *PLoS ONE* **2017**, *12*, e0190313. [CrossRef]

20. Fu, Y.H.; Zhou, X.; Li, X.; Zhang, Y.; Geng, X.; Hao, F.; Zhang, X.; Hanninen, H.; Guo, Y.; De Boeck, H.J.; et al. Decreasing control of precipitation on grassland spring phenology in temperate China. *Glob. Ecol. Biogeogr.* **2020**, *30*, 490–499. [CrossRef]

21. Ren, S.; Yi, S.; Peichl, M.; Wang, X. Diverse Responses of Vegetation Phenology to Climate Change in Different Grasslands in Inner Mongolia during 2000–2016. *Remote Sens.* **2017**, *10*, 17. [CrossRef]

22. Li, X.; Fu, Y.H.; Chen, S.; Xiao, J.; Yin, G.; Li, X.; Zhang, X.; Geng, X.; Wu, Z.; Zhou, X.; et al. Increasing importance of precipitation in spring phenology with decreasing latitudes in subtropical forest area in China. *Agric. For. Meteorol.* **2021**, *304–305*, 108427. [CrossRef]

23. Fu, Y.H.; Zhao, H.; Piao, S.; Peaucelle, M.; Peng, S.; Zhou, G.; Ciais, P.; Huang, M.; Menzel, A.; Penuelas, J.; et al. Declining global warming effects on the phenology of spring leaf unfolding. *Nature* **2015**, *526*, 104–107. [CrossRef] [PubMed]

24. Yuan, Z.; Bao, G.; Dorjsuren, A.; Oyont, A.; Chen, J.; Li, F.; Dong, G.; Guo, E.; Shao, C.; Du, L. Climatic Constraints of Spring Phenology and Its Variability on the Mongolian Plateau From 1982 to 2021. *J. Geophys. Res. Biogeosciences* **2024**, *129*, e2023JG007689. [CrossRef]

25. He, Z.; Du, J.; Chen, L.; Zhu, X.; Lin, P.; Zhao, M.; Fang, S. Impacts of recent climate extremes on spring phenology in arid-mountain ecosystems in China. *Agric. For. Meteorol.* **2018**, *260–261*, 31–40. [CrossRef]

26. Ma, X.; Huete, A.; Moran, S.; Ponce-Campos, G.; Eamus, D. Abrupt shifts in phenology and vegetation productivity under climate extremes. *J. Geophys. Res. Biogeosciences* **2015**, *120*, 2036–2052. [CrossRef]

27. Piao, S.; Tan, J.; Chen, A.; Fu, Y.H.; Ciais, P.; Liu, Q.; Janssens, I.A.; Vicca, S.; Zeng, Z.; Jeong, S.J.; et al. Leaf onset in the northern hemisphere triggered by daytime temperature. *Nat. Commun.* **2015**, *6*, 6911. [CrossRef]

28. Ji, S.; Ren, S.; Li, Y.; Dong, J.; Wang, L.; Quan, Q.; Liu, J. Diverse responses of spring phenology to preseason drought and warming under different biomes in the North China Plain. *Sci. Total Environ.* **2021**, *766*, 144437. [CrossRef]

29. Javed, T.; Li, Y.; Feng, K.; Ayantobo, O.O.; Ahmad, S.; Chen, X.; Rashid, S.; Suon, S. Monitoring responses of vegetation phenology and productivity to extreme climatic conditions using remote sensing across different sub-regions of China. *Environ. Sci. Pollut. Res. Int.* **2021**, *28*, 3644–3659. [CrossRef]

30. Yuan, M.; Zhao, L.; Lin, A.; Wang, L.; Li, Q.; She, D.; Qu, S. Impacts of preseason drought on vegetation spring phenology across the Northeast China Transect. *Sci. Total Environ.* **2020**, *738*, 140297. [CrossRef]

31. John, R.; Chen, J.; Ou-Yang, Z.-T.; Xiao, J.; Becker, R.; Samanta, A.; Ganguly, S.; Yuan, W.; Batkhishig, O. Vegetation response to extreme climate events on the Mongolian Plateau from 2000 to 2010. *Environ. Res. Lett.* **2013**, *8*, 035033. [CrossRef]

32. Li, C.; Filho, W.L.; Wang, J.; Yin, J.; Fedoruk, M.; Bao, G.; Bao, Y.; Yin, S.; Yu, S.; Hu, R. An assessment of the impacts of climate extremes on the vegetation in Mongolian Plateau: Using a scenarios-based analysis to support regional adaptation and mitigation options. *Ecol. Indic.* **2018**, *95*, 805–814. [CrossRef]

33. Rihan, W.; Zhao, J.; Zhang, H.; Guo, X. Preseason drought controls on patterns of spring phenology in grasslands of the Mongolian Plateau. *Sci. Total Environ.* **2022**, *838*, 156018. [CrossRef] [PubMed]

34. Luo, M.; Meng, F.; Sa, C.; Duan, Y.; Bao, Y.; Liu, T.; De Maeyer, P. Response of vegetation phenology to soil moisture dynamics in the Mongolian Plateau. *Catena* **2021**, *206*, 105505. [CrossRef]

35. Mei, L.; Bao, G.; Tong, S.; Yin, S.; Bao, Y.; Jiang, K.; Hong, Y.; Tuya, A.; Huang, X. Elevation-dependent response of spring phenology to climate and its legacy effect on vegetation growth in the mountains of northwest Mongolia. *Ecol. Indic.* **2021**, *126*, 107640. [CrossRef]

36. Bao, G.; Jin, H.; Tong, S.; Chen, J.; Huang, X.; Bao, Y.; Shao, C.; Mandakh, U.; Chopping, M.; Du, L. Autumn Phenology and Its Covariation with Climate, Spring Phenology and Annual Peak Growth on the Mongolian Plateau. *Agric. For. Meteorol.* **2021**, *298–299*, 108312. [CrossRef]

37. Wang, M.; Zhang, H.; Wang, B.; Wang, Q.; Chen, H.; Gong, J.; Sun, M.; Zhao, J. The Sensitivity of Green-Up Dates to Different Temperature Parameters in the Mongolian Plateau Grasslands. *Remote Sens.* **2023**, *15*, 3830. [CrossRef]

38. Li, G.; Yu, L.; Liu, T.; Bao, Y.; Yu, J.; Xin, B.; Bao, L.; Li, X.; Chang, X.; Zhang, S. Spatial and temporal variations of grassland vegetation on the Mongolian Plateau and its response to climate change. *Front. Ecol. Evol.* **2023**, *11*, 1067209. [CrossRef]

39. Bao, G.; Bao, Y.; Sanjjava, A.; Qin, Z.; Zhou, Y.; Xu, G. NDVI-indicated long-term vegetation dynamics in Mongolia and their response to climate change at biome scale. *Int. J. Climatol.* **2015**, *35*, 4293–4306. [CrossRef]

40. Bayarsaikhan, S.; Mandakh, U.; Dorjsuren, A.; Batsaikhan, B.; Bao, Y.; Adiya, Z.; Myagmartseren, P. Variations of Vegetation Net Primary Productivity and Its Responses to Climate Change from 1982 to 2015 in Mongolia. *ISPRS Ann. Photogramm. Remote Sens. Spat. Inf. Sci.* **2020**, *V-3-2020*, 347–353. [CrossRef]

41. Bao, G.; Tuya, A.; Bayarsaikhan, S.; Dorjsuren, A.; Mandakh, U.; Bao, Y.; Li, C.; Vanchindorj, B. Variations and climate constraints of terrestrial net primary productivity over Mongolia. *Quat. Int.* **2020**, *537*, 112–125. [CrossRef]

42. Meng, X.; Gao, X.; Li, S.; Lei, J. Spatial and Temporal Characteristics of Vegetation NDVI Changes and the Driving Forces in Mongolia during 1982–2015. *Remote Sens.* **2020**, *12*, 603. [CrossRef]

43. Wang, M.; Wang, S.; Wang, J.; Yan, H.; Mickler, R.A.; Shi, H.; He, H.; Huang, M.; Zhou, L. Detection of positive gross primary production extremes in terrestrial ecosystems of China during 1982–2015 and analysis of climate contribution. *J. Geophys. Res. Biogeosciences* **2018**, *123*, 2807–2823. [CrossRef]

44. Menzel, A.; Seifert, H.; Estrella, N. Effects of recent warm and cold spells on European plant phenology. *Int. J. Biometeorol.* **2011**, *55*, 921–932. [CrossRef] [PubMed]

45. Hou, X.; Gao, S.; Niu, Z.; Xu, Z. Extracting grassland vegetation phenology in North China based on cumulative SPOT-VEGETATION NDVI data. *Int. J. Remote Sens.* **2014**, *35*, 3316–3330. [CrossRef]

46. He, G.; Li, Z. Asymmetry of Daytime and Nighttime Warming in Typical Climatic Zones along the Eastern Coast of China and Its Influence on Vegetation Activities. *Remote Sens.* **2020**, *12*, 3604. [CrossRef]

47. Fu, Y.S.; Campioli, M.; Vitasse, Y.; De Boeck, H.J.; Van den Berge, J.; AbdElgawad, H.; Asard, H.; Piao, S.; Deckmyn, G.; Janssens, I.A. Variation in leaf flushing date influences autumnal senescence and next year's flushing date in two temperate tree species. *Proc. Natl. Acad. Sci. USA* **2014**, *111*, 7355–7360. [CrossRef]

48. Davy, R.; Esau, I.; Chernokulsky, A.; Outten, S.; Zilitinkevich, S. Diurnal asymmetry to the observed global warming. *Int. J. Climatol.* **2017**, *37*, 79–93. [CrossRef]

49. Peng, S.; Piao, S.; Ciais, P.; Myneni, R.B.; Chen, A.; Chevallier, F.; Dolman, A.J.; Janssens, I.A.; Penuelas, J.; Zhang, G.; et al. Asymmetric effects of daytime and night-time warming on Northern Hemisphere vegetation. *Nature* **2013**, *501*, 88–92. [CrossRef]

50. Zeng, Z.; Wu, W.; Ge, Q.; Li, Z.; Wang, X.; Zhou, Y.; Zhang, Z.; Li, Y.; Huang, H.; Liu, G.; et al. Legacy effects of spring phenology on vegetation growth under preseason meteorological drought in the Northern Hemisphere. *Agric. For. Meteorol.* **2021**, *310*, 108630. [CrossRef]

51. Ge, W.; Han, J.; Zhang, D.; Wang, F. Divergent impacts of droughts on vegetation phenology and productivity in the Yungui Plateau, southwest China. *Ecol. Indic.* **2021**, *127*, 107743. [CrossRef]

52. Maherali, H.; Pockman, W.T.; Jackson, R.B. Adaptive Variation in the Vulnerability of Woody Plants to Xylem Cavitation. *Ecology* **2004**, *85*, 2184–2199. [CrossRef]

53. Craine, J.M.; Ocheltree, T.W.; Nippert, J.B.; Towne, E.G.; Skibbe, A.M.; Kembel, S.W.; Fargione, J.E. Global diversity of drought tolerance and grassland climate-change resilience. *Nat. Clim. Chang.* **2012**, *3*, 63–67. [CrossRef]

54. Sun, Z.; Wang, Q.; Xiao, Q.; Batkhishig, O.; Watanabe, M. Diverse Responses of Remotely Sensed Grassland Phenology to Interannual Climate Variability over Frozen Ground Regions in Mongolia. *Remote Sens.* **2014**, *7*, 360–377. [CrossRef]

55. Wolf, S.; Eugster, W.; Ammann, C.; Häni, M.; Zielis, S.; Hiller, R.; Stieger, J.; Imer, D.; Merbold, L.; Buchmann, N. Contrasting response of grassland versus forest carbon and water fluxes to spring drought in Switzerland. *Environ. Res. Lett.* **2013**, *8*, 035007. [CrossRef]

56. Wu, X.; Liu, H.; Li, X.; Ciais, P.; Babst, F.; Guo, W.; Zhang, C.; Magliulo, V.; Pavelka, M.; Liu, S.; et al. Differentiating drought legacy effects on vegetation growth over the temperate Northern Hemisphere. *Glob. Chang. Biol.* **2018**, *24*, 504–516. [CrossRef]

57. Dantec, C.F.; Vitasse, Y.; Bonhomme, M.; Louvet, J.M.; Kremer, A.; Delzon, S. Chilling and heat requirements for leaf unfolding in European beech and sessile oak populations at the southern limit of their distribution range. *Int. J. Biometeorol.* **2014**, *58*, 1853–1864. [CrossRef]

58. Zheng, Z.; Zhu, W.; Chen, G.; Jiang, N.; Fan, D.; Zhang, D. Continuous but diverse advancement of spring-summer phenology in response to climate warming across the Qinghai-Tibetan Plateau. *Agric. For. Meteorol.* **2016**, *223*, 194–202. [CrossRef]

59. Li, X.; Guo, W.; Li, S.; Zhang, J.; Ni, X. The different impacts of the daytime and nighttime land surface temperatures on the alpine grassland phenology. *Ecosphere* **2021**, *12*, e03578. [CrossRef]

60. Shen, M.; Piao, S.; Chen, X.; An, S.; Fu, Y.H.; Wang, S.; Cong, N.; Janssens, I.A. Strong impacts of daily minimum temperature on the green-up date and summer greenness of the Tibetan Plateau. *Glob. Chang. Biol.* **2016**, *22*, 3057–3066. [CrossRef]

61. Crabbe, R.A.; Dash, J.; Rodriguez-Galiano, V.F.; Janous, D.; Pavelka, M.; Marek, M.V. Extreme warm temperatures alter forest phenology and productivity in Europe. *Sci. Total Environ.* **2016**, *563–564*, 486–495. [CrossRef]

62. Yin, P.; Li, X.; Pellikka, P. Asymmetrical Impact of Daytime and Nighttime Warming on the Interannual Variation of Urban Spring Vegetation Phenology. *Earth's Future* **2024**, *12*, e2023EF004127. [CrossRef]

63. Chen, X.; An, S.; Inouye, D.W.; Schwartz, M.D. Temperature and snowfall trigger alpine vegetation green-up on the world's roof. *Glob. Chang. Biol.* **2015**, *21*, 3635–3646. [CrossRef]

64. Schenk, H.J.; Jackson, R.B. Rooting depths, lateral root spreads and below-ground/above-ground allometries of plants in water-limited ecosystems. *J. Ecol.* **2002**, *90*, 480–494. [CrossRef]

65. Vitasse, Y.; Lenz, A.; Korner, C. The interaction between freezing tolerance and phenology in temperate deciduous trees. *Front. Plant Sci.* **2014**, *5*, 541. [CrossRef]

66. Scherrer, D.; Körner, C. Topographically controlled thermal-habitat differentiation buffers alpine plant diversity against climate warming. *J. Biogeogr.* **2011**, *38*, 406–416. [CrossRef]
67. Choukri, H.; Hejjaoui, K.; El-Baouchi, A.; El Haddad, N.; Smouni, A.; Maalouf, F.; Thavarajah, D.; Kumar, S. Heat and Drought Stress Impact on Phenology, Grain Yield, and Nutritional Quality of Lentil (*Lens culinaris* Medikus). *Front. Nutr.* **2020**, *7*, 596307. [CrossRef]
68. Li, J.; Bevacqua, E.; Chen, C.; Wang, Z.; Chen, X.; Myneni, R.B.; Wu, X.; Xu, C.-Y.; Zhang, Z.; Zscheischler, J. Regional asymmetry in the response of global vegetation growth to springtime compound climate events. *Commun. Earth Environ.* **2022**, *3*, 123. [CrossRef]